https://doi.org/10.5194/cp-2020-161
Preprint. Discussion started: 11 January 2021

Climate of the Past Discussions

Hydroclimatic variability of opposing late Pleistocene climates in the Levant revealed by deep Dead Sea sediments

Yoav Ben Dor[1], Francesco Marra[1,2], Moshe Armon[1], Yehouda Enzel[1], Efrat Morin[1]

[1] The Fredy and Nadine Herrmann Institute of Earth Sciences, The Hebrew University of Jerusalem, Jerusalem, 9190501, Israel
[2] Institute of Atmospheric Sciences and Climate, National Research Council of Italy, Bologna, 40129, Italy

Correspondence to: Yoav Ben Dor (Yoav.Bendor1@mail.huji.ac.il)

Abstract. Annual and decadal-scale hydroclimatic variability is a key characteristic embedded into climate insitu. It is therefore crucial to study hydroclimatic variability in order to understand its effects on climate derivatives such as hydrological processes and water availability. However, the study of this variability from modern records is limited due to their relatively short span, whereas model simulations relaying on modern dynamics could miss some of its aspects. Here we study annual to decadal hydroclimatic variability in the Levant using two sedimentary sections covering ~700 years deposited at ~18 and 27~ Ka retrieved from the depocenter of the Dead Sea, which has been continuously recording environmental conditions throughout the late Pleistocene. We focus on two ~700 years long series of annually-deposited laminated intervals (i.e., varves) representing two episodes of opposing mean climates, deposited during lake level rise and fall at 27 and 18 Ka, respectively. These two series comprise alternations of authigenic aragonite precipitated during summer and flood-derived detrital laminae deposited during winter. Within this record, aragonite laminae serve as a proxy of annual inflow and epilimnion dilution, whereas detrital laminae comprise sub-laminae that record individual floods. The two series depict distinct characteristics with increased mean and variance of annual inflow and flood frequency during "wetter", with respect to the "dryer", conditions. In addition, decades of intense flood frequency are identified (e.g., clusters), suggesting shifts between centennial-scale climatic regimes, which are particularly pronounced during wetter, lake-rising conditions. The combined application of multiple time series analyses indicates that episodes of falling lake levels are characterized by multiple pronounced quasi-periodic components with periodicities of 2-4, 6-8 and ~12 years, whereas the rising lake level episode presents weaker, less-persistent periodical components with similar periodicities. Combining these observations with the modern synoptic-scale hydroclimatology indicates shifts in the dominance of key synoptic systems governing rainfall, annual inflow and flood frequency in the eastern Mediterranean over centennial time-scale.

1 Introduction

Human activity relies on stable availability of freshwater, which in turn stems from the interaction of climatic, environmental and hydrologic conditions. Water availability is particularly crucial in drylands, which cover significant portions of the Earth's surface and host nearly 20% of the world's population (Safriel et al., 2005). In these areas, hydroclimatic variability of seasonal,

https://doi.org/10.5194/cp-2020-161
Preprint. Discussion started: 11 January 2021


Climate of the Past Discussions

annual and decadal scales bear significant effects on water availability that could lead to water stress as population grows (Luck et al., 2015; Luo et al., 2015). It is thus crucial to configure how hydroclimatic variability in drylands and Mediterranean regions could be affected by climatic changes, similar to those humanity faces in the upcoming decades (Peleg et al., 2015; Seager et al., 2019; Zappa et al., 2015). However, because the high resolution measurements required to study hydroclimatic variability only span several decades, the interpretation and the quantification of relationships between trends, oscillations and transitional states, as well as their impact on the local water cycle, are still limited and debated (e.g., Morin, 2011; Serinaldi et al., 2018). Furthermore, the impacts of climate change on discrete and short-term phenomena such as individual storms and floods, is proving harder to determine from the available short records because the extent of available data does not adequately capture all possible diversity of hydroclimatic states (Armon et al., 2018; Greenbaum et al., 2010; Metzger et al., 2020; Tarolli et al., 2012). Palaeohydrologic records cover centennial and millennial intervals at various resolutions (e.g., Allen et al., 2020; Baker, 2008; Brauer et al., 2008; Redmond et al., 2002; Witt et al., 2016), and hence, could improve our understating of how climate change is locally manifested into short-term hydroclimatic variability (e.g., Ahlborn et al., 2018; Swierczynski et al., 2012). Nevertheless, this requires continuous high-resolution archives, which are rare, especially in sub-tropical arid regions (e.g., Zolitschka et al., 2015).

The subtropical Levant exhibits a sharp climatic gradient ranging from subhumid Mediterranean to hyperarid climatic zones, where slight modifications of global atmospheric circulation could severely impact the hydrological cycle and affect water availability (Fig. 1; e.g., Held and Soden, 2006; Luck et al., 2015; Shohami et al., 2011; Tamarin-Brodsky and Kaspi, 2017). Precipitation in the Levant is limited to the mild and wet winters, whereas summers are dry and hot (Kelley et al., 2012; Kushnir et al., 2017; Seager et al., 2019). These properties further obscure the impacts of climatic changes on intra- and inter-annual hydroclimatic variability in the wetter Mediterranean regions, as they ultimately stem from the characteristics and frequency of discrete extra-tropical Mediterranean cyclones (i.e., Mediterranean/Cyprus Lows; e.g., Campins et al., 2011; Flocas et al., 2010; Saaroni et al., 2010; Ziv et al., 2004).

In this study, we use two high-resolution sequences of annually-deposited laminations (i.e., varves) of the Dead Sea deep drilling project (DSDDP) obtained from the Dead Sea depocenter within the framework of the international continental scientific drilling program (ICDP; e.g., Neugebauer et al., 2014; Stein et al., 2011). These sequences are analyzed to determine hydroclimatic variability in the southern Levant under contrasting late Pleistocene global and regional climate changes, recorded by independently-determined lake level trends (i.e., mean "wetter" vs. "dryer" conditions; e.g., Bartov et al., 2003; Torfstein et al., 2013; Torfstein and Enzel, 2017). The segments were continuously sampled for thin-sections preparation, and analyzed using high-resolution microfacies and multiple time-series analyses in order to address the following questions: (a) Can any significant differences between the two studied episodes deposited during opposing mean climates be identified? (b) Do the series illustrate significant intra-series transitions indicative of hydroclimatic regime shifts? (c) Do the studied sequences (or parts of them) record any periodic components? (d) Do the identified periodic components (partially) resemble

https://doi.org/10.5194/cp-2020-161
Preprint. Discussion started: 11 January 2021


Climate of the Past Discussions

65 periodic of known global teleconnections (e.g., NAO, the North Atlantic Oscillation; Black, 2012; Seager et al., 2019)? i.e., can some aspects of the modern hydroclimatic variability assist in interpreting dominant aspects of hydroclimatic variability during past climate changes?

2 Geological, hydrological, and climatological settings

The Dead Sea is the latest of a waterbodies series filling the deepest depression on earth, along the central part of the Dead
70 Sea transform since the late Miocene (e.g., Garfunkel, 1981; Garfunkel and Ben-Avraham, 1996; Waldmann, 2017; Waldmann et al., 2017). Because level changes in the Dead Sea are directly tied with precipitation fluctuations over its watershed (e.g., Enzel et al., 2003; Morin et al., 2019), its reconstructed past lake levels were utilized as a "mega palaeo-rain gauge" (Enzel et al., 2003), recording the integrated impacts of environmental conditions and climate on watershed hydrology (Bartov et al., 2003; Bookman et al., 2006; Machlus et al., 2000; Morin et al., 2019; Torfstein and Enzel, 2017). These impacts are propagated
75 into the lake's sedimentary record by lithological transitions from sequences of alternating aragonite and detrital laminae that accumulate during high lake stands and positive water budget (e.g., Ben Dor et al., 2019; Neugebauer et al., 2014; Torfstein et al., 2013), to halite (e.g., Kiro et al., 2016; Palchan et al., 2017; Sirota et al., 2017) or gypsum are deposited during drawdowns and droughts (Torfstein et al., 2008).

80 It was suggested that the climatic gradient over the Dead Sea watershed has been similar since the late Pleistocene (Enzel et al., 2008). This has dictated water and sediment paths to the lake, where the main water source is the Mediterranean-climate zone at the watershed's northern region (Enzel et al., 2003; Ziv et al., 2006). In this northern part of the watershed, annual water supply largely depends on the spatiotemporal properties and frequency of extra-tropical winter cyclonic systems (i.e., Mediterranean cyclones; Campins et al., 2011; Goldreich et al., 2004; Saaroni et al., 2010). Detrital sediments are delivered
85 by flash floods (e.g., Nehorai et al., 2013) and debris flows (e.g., Ahlborn et al., 2018; David-Novak et al., 2004), which may result from both Mediterranean cyclones, active Red Sea troughs (Dayan and Morin, 2006; Kahana et al., 2002; Tsvieli and Zangvil, 2005), and the less frequent disturbances to the subtropical jet stream also known as Tropical Plumes (Armon et al., 2018; Enzel et al., 2012; Tubi and Dayan, 2014; Ziv, 2001). Thus, the annual accumulation of alternating authigenic aragonite and detrital laminae throughout the majority of marine isotope stage 2 (MIS2) was attributed to seasonal deposition under high
90 lake levels and wetter-than-current mean conditions (Begin et al., 1980; Ben Dor et al., 2019; Haase-Schramm et al., 2004), as later confirmed by the comparison of laminae counting and radiometric dating (Prasad et al., 2004). These sequences dominate the record of Lake Lisan, which was the late Pleistocene predecessor of the Dead Sea (Begin et al., 1980). In Lake Lisan, winter inflow was probably a dominant source for replenishing carbonate content in the carbonate-poor Dead Sea after aragonite precipitation took place during summer (Kolodny et al., 2005; Neev, 1963; Neev and Emery, 1967; Stein et al.,
95 1997), whilst delivering detrital material to the lake (Nehorai et al., 2013).

https://doi.org/10.5194/cp-2020-161
Preprint. Discussion started: 11 January 2021


Climate of the Past Discussions

Until recently, studies of the sedimentary record of the Dead Sea and its predecessors focused on available exposures surrounding the lake (e.g., Bartov et al., 2003, 2007; Prasad et al., 2004; Stein et al., 1997; Torfstein, 2008) and on short cores of Holocene sequences (e.g., Heim et al., 1997; Migowski et al., 2006). They were thus affected by local conditions and hiatuses when lake levels had fallen below the exposures' altitude (Machlus et al., 2000; Torfstein et al., 2009, 2013) or by wave erosion during episodes rising lake level. In addition, these exposures were accumulated on the lake's shelf, and they therefore reflect its shallow environment, whereas the deeper part of the lake remained nearly inaccessible except for short coring campaigns (e.g., Garber et al., 1987; Nissenbaum et al., 1972). The recently collected ICDP-DSDDP cores from the lake's depocenter, therefore, provide a new regional perspective on sedimentary, limnological and hydrological processes in the lake (e.g., Coianiz et al., 2019; Neugebauer et al., 2014). Detailed microfacies investigation of these cores revealed that the detrital laminae, which alternate with aragonite laminae, are comprised of multiple sub-laminae, each recording individual flood that reached the ICDP-DSDDP coring site from the eastern and western streams flowing to the lake (Ben Dor et al., 2018). Because the majority of these streams are ephemeral, and have relatively small watersheds (<1000 km^2), flash-floods may form both by regional precipitating storms and/or local convection. The laminated record of the deep ICDP-DSDDP core therefore provides a regional record of two independent hydroclimatological variables at annual resolution: (a) the thickness of aragonite laminae, and (b) the number of graded sub-laminae in the detrital layers. Although more recent investigations indicate that the aragonite laminae thickness are not linearly related to total annual inflow into the lake, as previously suggested by Stein et al., (1997), they are still correlated with dilution of the lake and bicarbonate content, and therefore still provide valuable insights on pacing, inherent periodicities and inter-annual inflow variability (Ben Dor et al., in review). The number of detrital sub-laminae in every detrital lamina, on the other hand, records the number of floods that managed to deliver detritus to the coring site, i.e., the floods exceeding some kind of threshold (Ben Dor et al., 2018).

https://doi.org/10.5194/cp-2020-161
Preprint. Discussion started: 11 January 2021

Climate of the Past
Discussions
Open Access
EGU

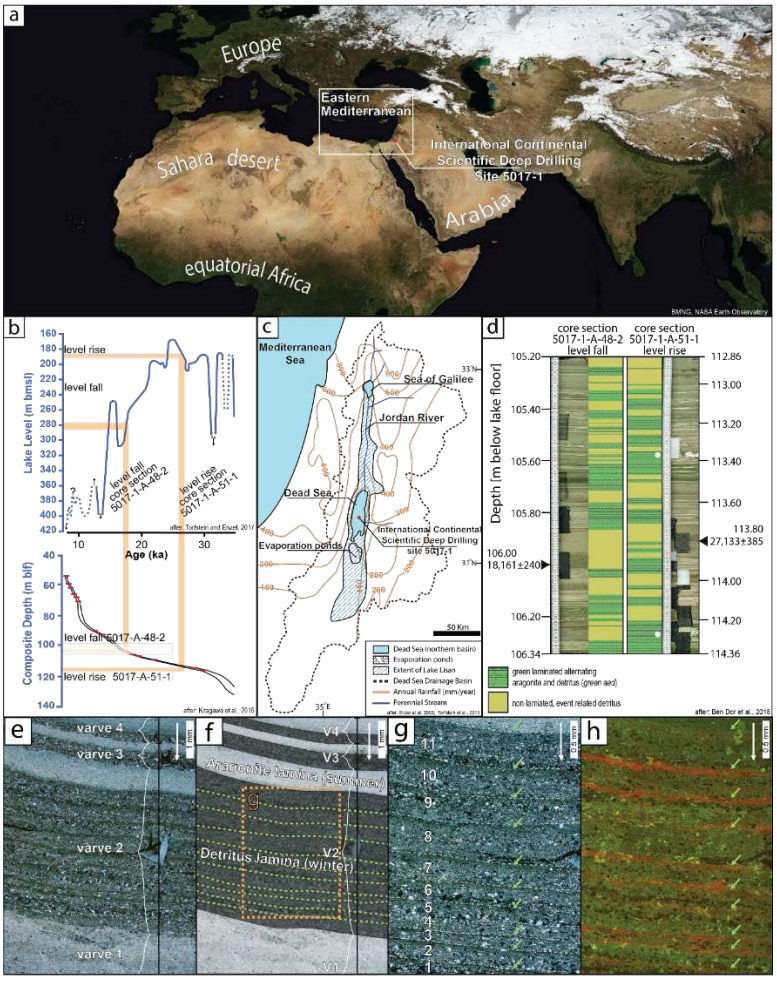

Figure 1: a) Satellite image of the Mediterranean and its surroundings depicting the pivotal location of the ICDP-DSDDP site 5017-1 on the seam of global climate belts (extracted from The Blue Marble Next Generation, NASA's Earth Observatory; Stöckli et al., 2005). b) Top: Dead Sea lake level curve between 10 and 40 Ka showing the high stage of Lake Lisan, the Late Pleistocene predecessor of the Dead Sea during the last glacial (marine isotope stage, MIS2, ~15-30 Ka) after Bartov et al., 2003 and Torftein and Enzel, 2017. Bottom: The age-depth model of the ICDP-DSDDP 5017-1 core and the respective position of the studied segments along the core (after Kitagawa et al., 2017. c) The Dead Sea watershed and the geographic extent of Lake Lisan during the last glacial maximum plotted on modern precipitation isohyets (after Enzel et al., 2003 and Torfstein et al., 2013). d) The studied segments of the ICDP-DSDDP cores dated to 18Ka and 27Ka (MIS 2). e-h) Microscope images of alternating aragonite (summer precipitate) and detritus (deposited during winter) varves depicting a detrital laminae composed of multiple sub-laminae (labeled 1-11) deposited by individual floods.

https://doi.org/10.5194/cp-2020-161
Preprint. Discussion started: 11 January 2021


Climate of the Past Discussions

3 Materials and methods

3.1 Microfacies analyses

Two chronologically-constrained segments of the ICDP-DSDDP 5017-1 core were selected for this study (ca. 18 and 27 Ka; Fig. 1; Neugebauer et al., 2014). These segments are coeval with opposing climatic trends, reflected by independently-determined rising (27 Ka) and falling (18 Ka) lake level trends (Fig. 1b; Bartov et al., 2002; Torfstein and Enzel, 2017). Continuous thin sections were prepared using a procedure adjusted for saline sediments (e.g., Brauer et al., 1999; Neugebauer et al., 2015), and analyzed using a Hirox RH-2000 optical microscope. A total of ~700 varves (years) were counted and described in each segment (Fig. S1). The segments comprise alternations of finely laminated varves (Ben Dor et al., 2019) and event-related deposits (ERDs; Neugebauer et al., 2014), attributed to debris flows (Ahlborn et al., 2018) and earthquakes (Kagan et al., 2018). This study focuses on two properties of the varves interpreted as hydrological proxies: (a) the thicknesses of aragonite laminae, and (b) the number of detrital sub-laminae in each detrital lamina (Figs. 1 and 2). Because the thickness of detrital laminae cannot be directly linked to specific hydroclimatic aspects, but instead depends on the interaction of multiple factors such as sediment availability and the location of the activated catchment, it is not analyzed here as a hydroclimatic proxy. The thickness of aragonite laminae was suggested to reflect annual inflow and lake dilution during the wet season (Kolodny et al., 2005; Stein et al., 1997), whereas individual sub-laminae in detrital laminae correspond to flood events capable of delivering siliciclastic sediments to the coring site (Ben Dor et al., 2018). These sub-laminae are attributed to floods that surpassed the threshold required to reach the coring site from their catchments. Missing data, such as were laminae are trimmed or distorted (~5%) were completed by median values prior to time-series analyses.

We note that because the typical number of sub-laminae is low, and the minimal number of detrital sub-laminae that can be counted is one, as no cases of "zero sub-laminae" are sedimentologically-distinguishable, varves comprising a single detrital lamina should be considered as varves recording either years with no floods or years with a single flood. The two series deposited during rising and falling lake levels were compared using key statistical properties: the Mann-Whitney-Wilcoxon ranksum test to determine if they were sampled from two populations of a statistically different median (MWW; Mann and Whitney, 1947), and the Ansari-Bradley (1960) ranksum dispersion test to determine if they were characterized by statistically significant dispersion.

3.2 Detecting intra-record regime shifts

Regime shifts were identified using a non-parametric test that utilizes the normalized running sum as the test statistic was developed for identifying flood-rich episodes (i.e., clusters; Appendix B) and refined using a running MWW and Ansari-Bradley tests (Figs. S2 and S3). Following a visual inspection, the tests were applied with a symmetric window of 51 years width (25 years in each direction), that was adequate for this purpose by visual inspection. First, the running sum of sub-laminae was calculated for each series using multiple equally-spaced window widths ranging from 10 to 300 years. The running

https://doi.org/10.5194/cp-2020-161
Preprint. Discussion started: 11 January 2021

sum was consequently normalized to its mean value for every window width, and peaks in the series were identified. In order to avoid overlaps, only local maximum values, separated by at least half window width, were further considered for the analysis (Figs. S2-1 and S2-6). The peaks were ordered according to their rank in descending order, where the largest value was assigned the first position and the smallest value was assigned the last position. Each of the original data series was then randomly permutated 10,000 times without replacement and the same statistics (peaks of normalized running-sum) were calculated. This resulted in a large dataset of values for the peaks of normalized running-sum, allowing the calculation of their distributions, and the estimation of the likelihood of randomly observing such values (Figs. S2-2 and S2-7). The observed value of the normalized running sum for every peak rank and window width was compared to the distribution derived from the 10,000 randomly permutated series (Figs. S2-3 and S2-8). Observed values larger than the 95th percentile are hereby considered statistically significant with a false positive error of 0.05 (Figs. S2-4 and S2-9). Because of the wide range of applied window widths for the statistical test, the significant peaks of different widths tend to overlap each other, so the clusters were eventually evaluated by considering their summed probabilities (Figs. S2-5 and S2-10), and their edges were further refined by a running MWW test.

Recurrence and cross-recurrence analyses were applied to identify non-linear transitions and distinct regimes (Eckmann et al., 1987). These methods can be used to detect abrupt transitions as well as short-term periodic and quasi-periodic behaviors in non-stationary and noisy series by investigating their dynamics in the reconstructed phase space (Donges et al., 2011; Marwan et al., 2007). This approach is specifically useful in this study because the studied proxies record the convolved non-linear interaction of climatic, hydrological and limnogeological processes. Because the effect of their interactions could stem from non-linear dynamics that bear different implications on the studied sedimentary sections, the application of recurrence-based methods could prove more robust than specific harmonic or wavelet functions (Marwan et al., 2003; Marwan and Kurths, 2004). The analysis was carried out using the CRP toolbox for MATLAB© after normalizing the series to zero mean and unit standard deviation (ver. 5.22; Marwan et al., 2007). The embedding dimension and the time-delay were determined using the false nearest neighbor approach (Kennel et al., 1992) and the mutual information method (Fig. S4; Marwan, 2011), respectively. An environment of uniform size was selected by a visual inspection of the plots ($\varepsilon=1\sigma$ for recurrence and $\varepsilon=1.5\sigma$ for joint-recurrence analyses). Recurrence quantification analysis (RQA) was used to calculate the recurrence rate (RR) and the transitivity coefficient, which describe the degree of regularity of the system's dynamics using the recurrence plot (Marwan et al., 2007), using a 30-years moving window with 20% overlap, which were found to be informative and not too noisy for this purpose.

3.3 Detecting periodical components

Hydrological data are usually not normally distributed, and may show short-term periodicities that would be hard to identify using standard Fourier-derived approaches such as the periodogram (Blackman and Tukey, 1958; e.g., Welch, 1967). Wavelet analyses provide a flexible tool for identifying irregular and non-stationary periodicities in short time series (Lau and Hengyi

https://doi.org/10.5194/cp-2020-161
Preprint. Discussion started: 11 January 2021


Climate of the Past Discussions

Weng, 1995; Torrence and Compo, 1998). We utilized the principles delineated by Torrence and Compo (1998) using the Morlet wavelet function after normalizing the data to zero mean and unit standard deviation (Grinsted et al., 2004). Significance testing was carried out against simulated red noise modeled by a lag-1 autoregressive process (AR(1); Grinsted et al., 2004; Torrence and Compo, 1998).

Singular spectrum analysis (SSA) is used to identify periodic and quasi-periodic signals in short, non-stationary and noisy time series (Broomhead and King, 1986). Unlike wavelet and Fourier-based procedures, where the signal is compared against a predefined function, SSA identifies key components that best explain the variance of the time-delayed series in an embedding matrix. This non-parametric approach reveals the dominant components that best explain data variance and defines their relative contribution for generating the observed signal (Vautard and Ghil, 1989). This, in turn, allows the breaking-down of the signal into its principle components and calculating their corresponding reconstructed components (RCs), which demonstrate the extent of contribution for each component to the signal (Ghil et al., 2002). Thus, the analyses of the individual RCs, and the determination of their dominant periodicities can point to dominant frequencies embedded in the observed series, which in turn could stem from teleconnections affecting hydroclimatic variability (e.g., NAO, SOI, etc.; Feliks et al., 2010; Le Mouël et al., 2019; Seager et al., 2019). To balance between the analyses complexity and usefulness, and avoid overfitting of the SSA, it was performed with an embedding dimension (window) of ten years after visually inspecting the effect of RC number of the eigenvalues. The first RC ($RC^{(1)}$) was later used as the local trend component that was subtracted from the data as a high-pass filter to reveal short-term periodicities (Fig. S5). The SSA RCs were additionally analyzed using Welch's periodogram for evaluating the RCs power spectral density (Welch, 1967), and wavelet and cross-wavelet analyses (Grinsted et al., 2004) in order to identify their dominant periodicities in cluster and the background periods. The periodogram was calculated after applying a Hamming window of width 25 years and an overlap of 50%, applied to merge close periodical components and reduce spectral noise, after subtracting the mean from the series and zero-padding it to 2^{11} points in order to minimize spectral leakage (Figs. S7-S11). Additionally, a multi-channel SSA (Groth and Ghil, 2015) followed with a cross-wavelet and Welch's periodogram analyses was performed (Figs. S12 and S13).

4 Results

4.1 Microfacies analyses

The studied segments are dominated by alternating laminae of aragonite and detritus with a greenish tint (Figs. 1, S1) characterized by a typical laminae thickness of <1 mm. The laminated segments are sporadically interrupted by massive or graded ERDs attributed to abrupt mass wasting events (e.g., turbidities and slumps), likely triggered by earthquakes (Kagan et al., 2018), debris flows and slope instability (Ahlborn et al., 2018). Both laminae thickness and number of sub-laminae show

https://doi.org/10.5194/cp-2020-161
Preprint. Discussion started: 11 January 2021


Climate of the Past Discussions

225 statistically significant larger mean and variance during lake level rise (~27 Ka) than during lake level fall (~18Ka; Table 1; Fig. 2).

Aragonite laminae thicknesses ranges between 51 and 2259 μm (μ=457μm, σ=308 μm), and 53 and 6,020 μm (μ=642 μm, σ=529 μm) in the falling and rising segments, respectively. Detrital laminae thicknesses range from 27 to 13,136 μm
230 (μ=312μm σ=638 μm), and 27 and 8,760 μm (μ=416 μm, σ=675 μm) in the falling and rising segments, respectively. The number of sub-laminae during the falling lake level ranges between 1 and 10 (μ=1.2, σ=0.7), and between 1 and 17 (μ=1.6, σ=1.6) in the rising lake level, respectively (Table 1). The MWW test indicates a significant difference between all studied proxies when comparing the two studied series (p value <<0.05). The difference in dispersions of all variables between rising and falling lake levels are statistically significant (p value<<0.05) except for detrital laminae, where the Ansari-Bradley test
235 failed to reject the null hypothesis (p value≈0.12). All three parameters show positive skewness of 2.1 and 3.5 for aragonite laminae thickness, 12.7 and 7.6 for detrital aragonite laminae, and 5.9 and 6.1 of the number of sub-laminae in falling and rising lake levels, respectively. No substantially significant correlation exists between any two of the parameters in each time series, with the exception of a moderate correlation between the number of sub-laminae in the detrital laminae and laminae thickness (Fig. 3; r=0.52 and 0.61, for falling and rising lake levels, respectively; with p values <<0.005).

240

Table 1 – Bulk statistical properties of the studied sedimentary series.

Rise/fall	Parameter	Unit	Min	Max	Median	Mean	Std. deviation	Skewness
fall	aragonite	μm	51	2259	388	457	308	2.1
fall	detritus	μm	27	13,136	164	312	638	12.7
fall	Number of detrital sub-laminae	count	1	10	1.0	1.2	0.7	5.9
rise	aragonite	μm	53	6020	509	642	529	3.5
rise	detritus	μm	27	8760	262	416	675	7.6
rise	Number of detrital sub-laminae	count	1	17	1.0	1.6	1.6	6.1

https://doi.org/10.5194/cp-2020-161
Preprint. Discussion started: 11 January 2021

Climate of the Past Discussions

Table 2 – p values of the statistical comparison between the bulk studied series

Rise/fall	Parameter	Test[1]	p value[2]	Significant at α=0.05
fall	aragonite	MWW	< 0.001	Yes
fall	detritus	MWW	< 0.001	Yes
fall	Number of detrital sub-laminae	MWW	< 0.001	Yes
rise	aragonite	AB	0.001	Yes
rise	detritus	AB	0.120	No
rise	Number of detrital sub-laminae	AB	< 0.001	Yes

1 – MWW – Mann-Whitney-Wilcoxon ranksum test, AB – Ansari-Bradley dispersion test.
2 – tests with p values smaller than 0.05, are considered significant at α=0.05.

https://doi.org/10.5194/cp-2020-161
Preprint. Discussion started: 11 January 2021

Climate of the Past Discussions
Open Access
EGU

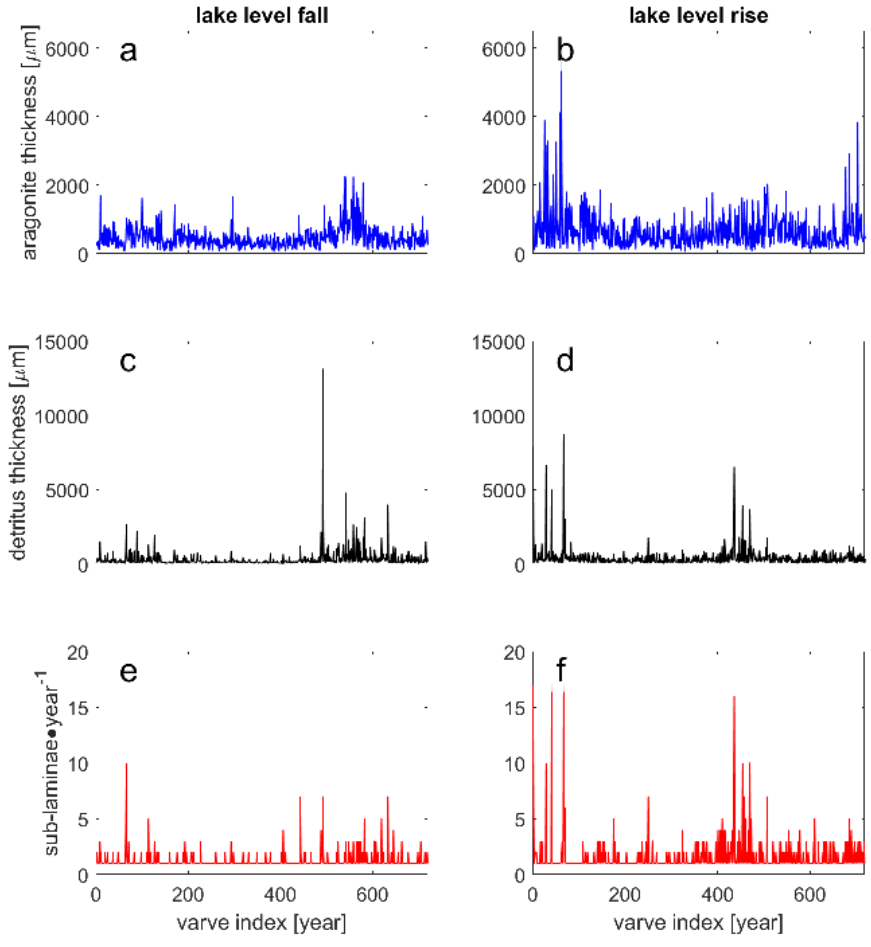

Figure 2 – Time series of microfacies analysis of the studied varved sections. (a, b; blue) aragonite laminae thickness, (c, d; black) detritus laminae thickness, (e, f; red) number of floods identified by modifying the number of counted detrital sub-laminae as described in the text.

https://doi.org/10.5194/cp-2020-161
Preprint. Discussion started: 11 January 2021

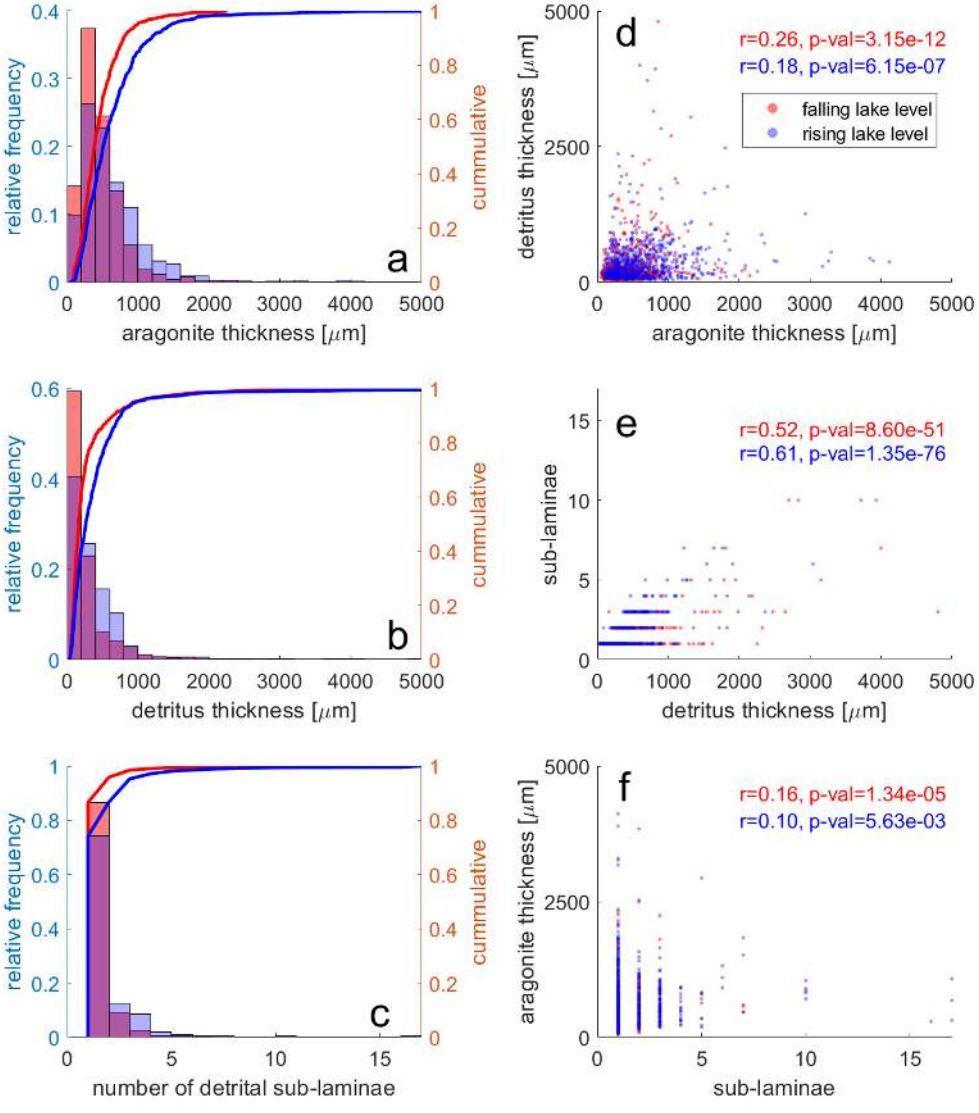

Figure 3 – Distributions and correlations of the trivariate geological time series showing the distributions of (a) aragonite laminae thickness, (b) detritus laminae thickness and c) number of sub-laminae counted in each detrital lamina. Plots d-f show the correlations between aragonite and detritus thickness (d, r^2=0.07, 0.03), number of floods and detritus thickness (e, r^2=0.27, 0.37), and number of floods and aragonite laminae thickness (f, r^2=0.03,0.01)

https://doi.org/10.5194/cp-2020-161
Preprint. Discussion started: 11 January 2021


Climate of the Past Discussions

4.2 Detecting intra-record regime shifts

Two clusters of intense flood frequency were identified in each of the studied series (Table 3). Although two clusters are identified, one of the clusters in each series appears more robust in comparison with the other, as it was identified using multiple window widths (Figs. S2-5 and S2-10). The clusters are labeled robust and less robust accordingly (Table 3). However, we note that this different robustness estimation could stem from an "edge effect" bias, that limits the analysis of segments close to the edges of the series using a large range of window widths. The recurrence analyses demonstrate a substantial drop in both recurrence rate and the transitivity coefficient at the beginning of all clusters, although the first, less robust cluster, also depicts a rise in both parameters after the initial drop, which testifies to the reduced robustness of its identification as a cluster (Fig. 4 and 5).

Table 3 – Identified clusters in the two studied series following the procedure Appendix B based on number of detrital sub-laminae.

	Level fall [index years]	Estimated robustness	Level rise [index years]	Estimated robustness
1st cluster	47-138	Less robust	1-83	Less robust
2nd cluster	519-662	Robust	394-534	Robust

https://doi.org/10.5194/cp-2020-161
Preprint. Discussion started: 11 January 2021

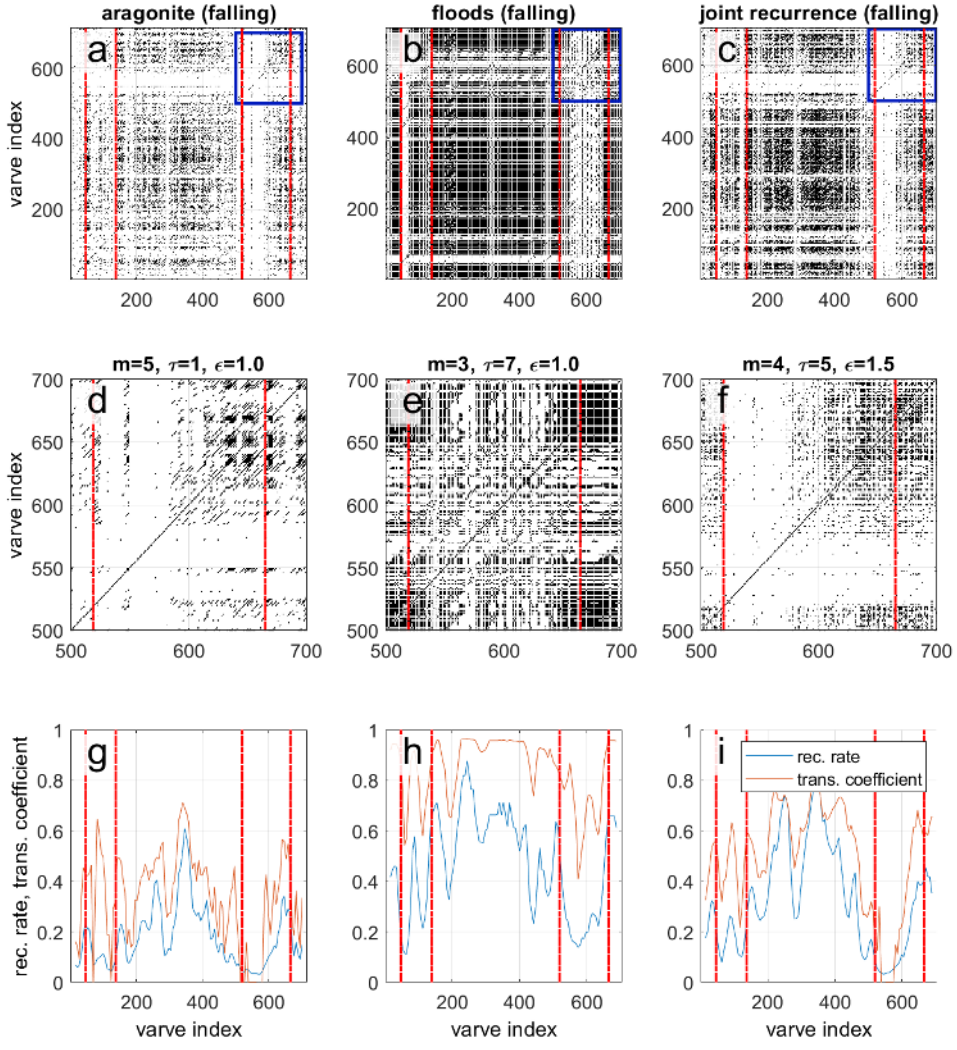

Figure 4 – Recurrence analyses of studied lake level fall depicting the recurrence plots for aragonite thickness (a), flood frequency (b) and the joint recurrence plot for the two proxies calculated using a maximum norm. Blue rectangle indicates the extent of data presented in (d-f). d-f depict a zoomed in segment of corresponding plots a-c. Note the parallel diagonal lines that characterize the aragonite thickness (a,d), and indicate an inherent quasi-periodic behaviour, whereas the flood series forms sporadic points and polygons that reflect a more cahotic or random beviour. g-i show the recurrence rate and the trasitivity coefficient over using a running window size of 30 years and 20% overlap. The analyses were carried over the detrended data using the SSA RC[(1)]. Selected parametrs for the embedding are m (dimension), τ (delay) and ε (threshold) used for space phase reconstructions are presented in the figure. Red lines represent possible cluster. Pronounced non-stationarity is shown by a sharp decrease in recurrence and transitivity prior and during the possibly identified cluster.

https://doi.org/10.5194/cp-2020-161
Preprint. Discussion started: 11 January 2021

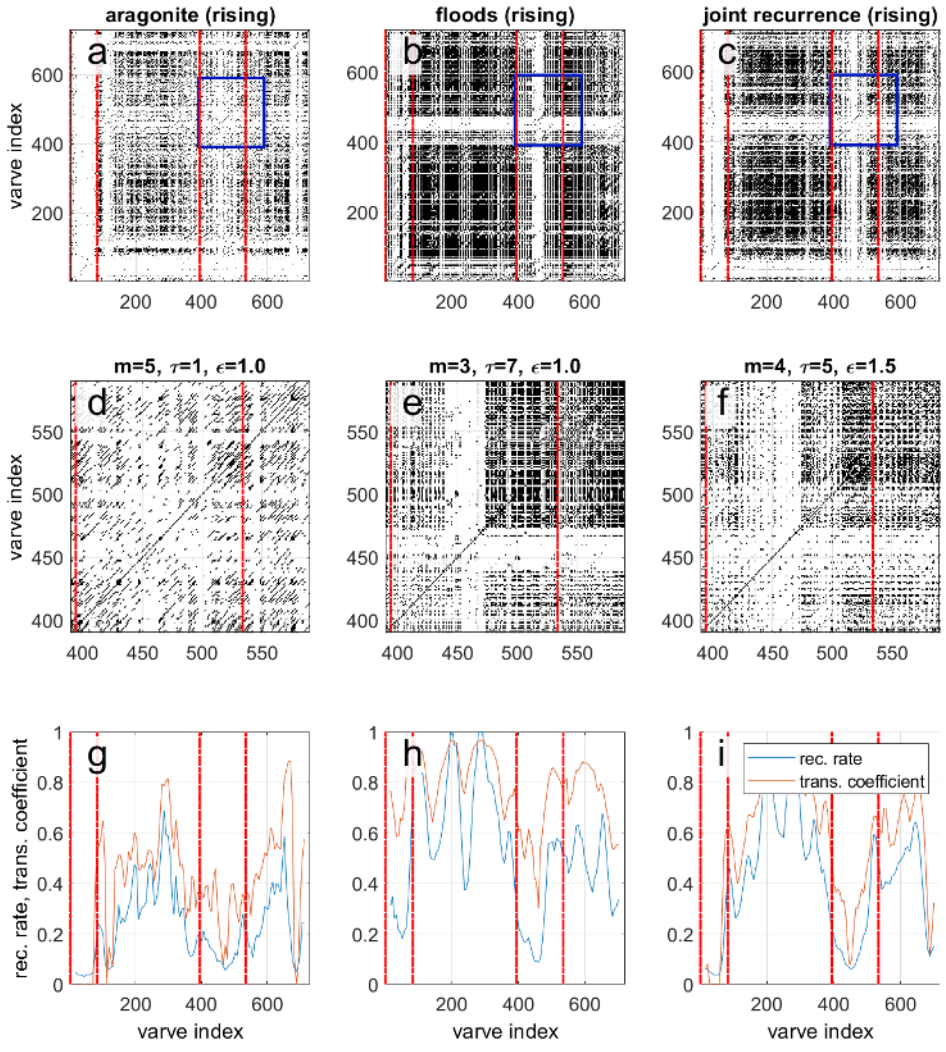

Figure 5 – Recurrence analyses of studied lake level rise depicting the recurrence plots for aragonite thickness (a), flood frequency (b) and the joint recurrence plot for the two proxies calculated using a maximum norm. Blue rectangle indicates the extent of data presented in (d-f). d-f illustrate zoomed in segment of the corresponding plots a-c. Note the parallel diagonal lines that characterize the aragonite thickness (a,d), and indicate an inherent quai-periodic behaviour, whereas the flood series forms sporadic points and polygons that reflect a more cahotic or random beviour. g-i show the recurrence rate and the trasitivity coefficient over using a running window size of 30 years and 20% overlap. The analyses were carried over the detrended data using the 1st SSA RC. Selected parametrs for the embedding are m (dimension), τ (delay) and ε (threshold) used for space phase reconstructions are presented in the figure. Red lines portray possible cluster. Pronounced non-stationarity is depicted by a sharp decrease in recurrence and transitivity prior and during the possibly identified cluster.

https://doi.org/10.5194/cp-2020-161
Preprint. Discussion started: 11 January 2021


Climate of the Past Discussions

4.2 Detecting periodical components

Recurrence analyses of aragonite thicknesses indicate periodic or quasi-periodic behaviours, reflected by the diagonal lines appearing throughout the recurrence plot of the series (Figs. 4a,4d and 5a,5d). Conversely, the flood frequency series present blocky and irregular patterns that indicate an underlying chaotic, random, or practically non-periodic process (Figs. 4b,4e and 5b,5e). In particular, the segments identified as clusters demonstrate decreased recurrence rate and transitivity, suggesting a shift in the system's dynamics, both in aragonite thickness and in the number of sub-laminae. Although this behavior is somewhat expected for the sub-laminae series that was used to determine clusters in the first place, it is also evident for the aragonite data.

Discontinuous short-term periodicities with a period ranging between two and eight years appear sporadically throughout the entire dataset in both aragonite and flood frequency series (Fig. 6). These short term oscillations fail the significance test of the global wavelet spectrum against an AR(1) red noise process, but appear to be significant in the analyses of the detrended data after subtracting $RC^{(1)}$ (Figs. S14), which may indicate that their importance could be obscured by contrasting trend components. A statistically significant centennial- to bicentennial-scale (~120-250 years) periodic component is observed in both aragonite thickness series, although its robustness is difficult to estimate as it falls largely outside the cone of influence. A similar periodic component is also identified in the sub-laminae series during lake level rise, but not in the interval of lake level fall.

https://doi.org/10.5194/cp-2020-161
Preprint. Discussion started: 11 January 2021

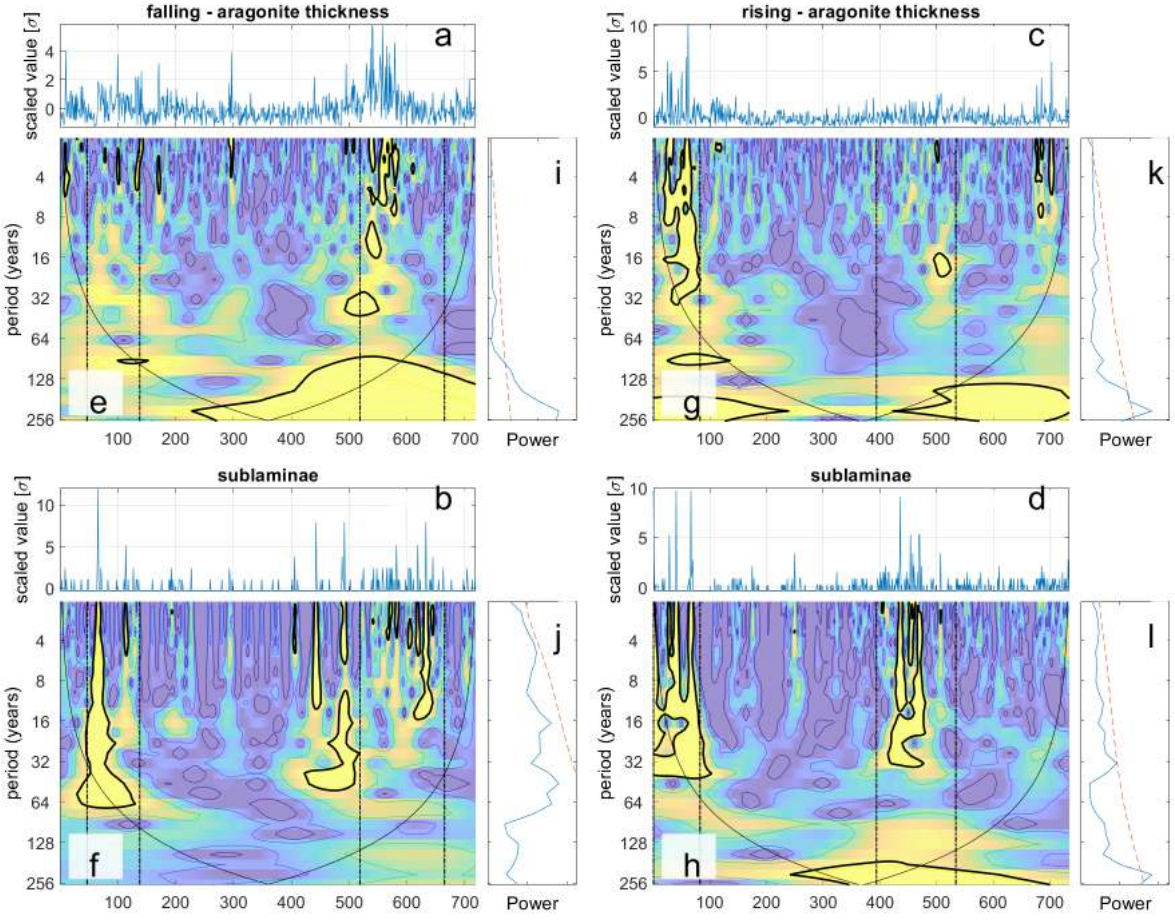

Figure 6 – Wavelet and global-wavelet spectra of aragonite thickness and flood frequency during falling (left) and rising (right) episodes. Periodicities with significance level above 0.95 (alpha=0.05) are depicted by a bold black line. Each triplot section shows the data after normalization (a-d), the wavelet spectra (e-h) and the global wavelet spectra (blue) compared against a background red noise estimate (dashed red, i-l) Vertical dashed lines depict clusters identified as episodes of increased flood frequency. Note the loss of significance of the short-term periodic component in the global wavelet spectra that is resolved in the analysis of the detrended series (Fig. S14)

The SSA RCs are characterized by multiple periodic components (Figs. S6-S11). The first two components are considered as the local trend component, and accordingly depict persistent "long-wave" periodic components with wave lengths >32 years. The following components show roughly three peaks characterized by periodicities of 2-3 years, 4-5 years, and 7-8 years. The multichannel SSA and its corresponding cross-wavelet analyses demonstrates that the periodic component with 4-5 years periodicity is relatively robust during lake level fall, but less persistent during lake level rise (Figs. S12 and S13).

https://doi.org/10.5194/cp-2020-161
Preprint. Discussion started: 11 January 2021


Climate of the Past Discussions

5 Discussion

5.1 The mechanistic link between mean properties and variability

Due to the unique hydroclimatic settings of the lake and its sedimentary record, the record cannot be directly interpreted from the perspective of a flood frequency analysis (e.g., Metzger et al., 2020), where the frequency and magnitude of floods in individual watersheds are studied. This is because the studied detrital sub-laminae in the ICDP-DSDDP core record the number of flood events (potentially lasting up to several days) that exceeded the threshold required to reach the coring site at the lake center (Ben Dor et al., 2018), instead of recording discharge properties at individual watersheds (Nehorai et al., 2013). Furthermore, the bathymetry of the basin dictates that only large-enough floods in tributaries, situated in front of the coring site on both sides of the escarpment, could have deposited detrital material at the coring site (Ben Dor et al., 2018; Nehorai et al., 2013). Although this aspect masks some delicate features that could otherwise be extracted in the analyses of modern measurements, its length and established context with respect to regional climatic conditions testifies to its value.

By assuming that the dominant synoptic-scale circulation patterns during the late Pleistocene resembles modern conditions in the region (Enzel et al., 2008), it can be argued that flood events recorded as detrital sub-laminae at the depocenter of Lake Lisan can result from three main synoptic circulation systems (e.g., Armon et al., 2019); the interplay between these three systems determines the mean climatic conditions (i.e., precipitation). Thus, the association of increased flood frequency with rising lake levels was initially interpreted as reflecting increased frequency and/or modulation of the track and depth of Mediterranean lows that deliver the majority of annual precipitation over the Dead Sea watershed (Ben Dor et al., 2018). However, a more detailed comparison of flood frequency with aragonite laminae thickness, that reflects annual inflow and dilution to some extent (Kolodny et al., 2005; Stein et al., 1997), reveals more subtle insights and a delicate interplay of hydroclimatic factors manifested through the watershed during opposing climatic regimes.

Both aragonite laminae thickness and flood frequency have larger mean and variance during lake level rise (Table 1). Because rising lake levels indicate a “wetter” climate on average, this relationship between mean and variance is similar to this relationship observed in modern precipitation (e.g., Morin et al., 2019). This relationship, thus, strengthens the interpretation of these sedimentary proxies as hydroclimatic proxies. Namely, the increased thickness of aragonite laminae and the increased number of detrital sub-laminae, in detrital laminae containing more than one sub-laminae, suggests that the episodes of rising lake level were characterized both by increased annual inflow and increased frequency of floods. As suggestions invoking increased flood frequency were raised both for wetter and drier conditions were made (e.g., Alpert et al., 2002; Rohling, 2013; Yosef et al., 2019), this observation demonstrates that increased frequency of floods during wetter intervals in Mediterranean climate zone is the likely scenario. Furthermore, the coupling of increased observed increased thickness of aragonite laminae with increased flood frequency may support their interpretation by a common hydroclimatic mechanism, such as the increased

https://doi.org/10.5194/cp-2020-161
Preprint. Discussion started: 11 January 2021

Climate of the Past Discussions

occurrence of Mediterranean low pressure systems, suggested by earlier studies (Armon et al., 2019; Ben Dor et al., 2018; Enzel et al., 2008).

5.3 Periodical components and variability pacing

One of the goals in studying hydroclimatological proxies is identifying key periodical components that pace short-term variability under different mean climatic regimes (e.g., Ghil et al., 2002; Grinsted et al., 2004). Because (a) the thickness of aragonite laminae was suggested to reflect annual hydroclimatic conditions (Kolodny et al., 2005), and (b) periodicities attributed to solar cycles were previously identified by spectral analyses of laminae thickness at the exposed coeval MIS2 White Cliff Member of the Lisan Formation at Masada (Prasad et al., 2004), a similar attempt was made in this study as well. Prasad et al., (2004) report periodicities of 50-60 years, similar to those identified here (Figs. 7, S12 and S13). Additionally, wavelet analyses of previously reported $\delta^{18}O$ and $\delta^{13}C$ from ~200 aragonite laminae recovered from MIS2 exposures of the Lisan Formation at Masada and Perazim Valley were hereby conducted. Because the systematics of these isotopic compositions are distinctly different, these proxies bear different implication on environmental conditions in the lake and its surroundings. More specifically, $\delta^{18}O$ is directly influenced by hydroclimatology, whereas $\delta^{13}C$ is primarily affected by biological activity (Kolodny et al., 2005). Nevertheless, it appears that because the extent of biological activity in the saline Lake Lisan depended on freshwater inflow that also replenished its surface water with required nutrients (Begin et al., 2004), the two proxies seem to share similar pacing and are broadly characterized by non-persistent periodical components of 2-6 years (Fig. 7), similar to those observed in the deep core (Fig. 6).

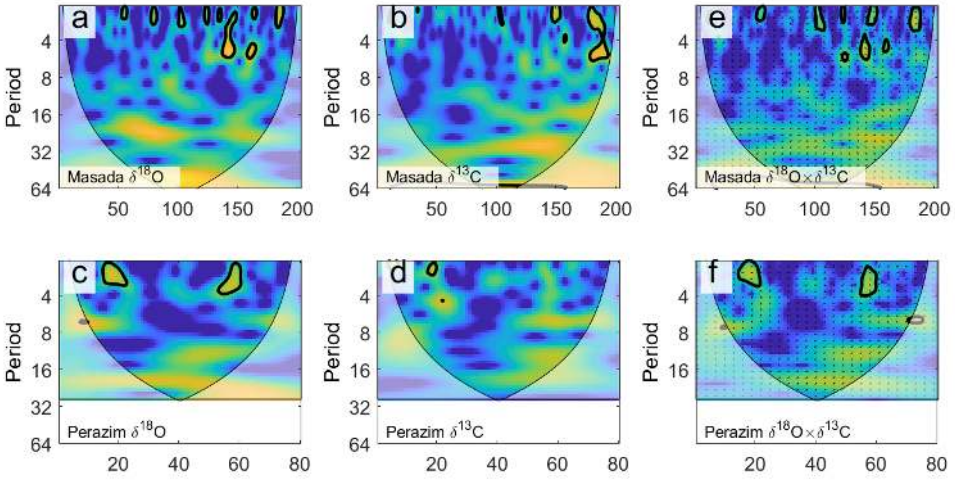

Figure 7 – Wavelet (a-d) and cross-wavelet analyses of $\delta^{18}O$ and $\delta^{13}C$ in two segments of the Masada (30 Ka) and Perazim (25 Ka) exposures of the White Cliff Member (Lisan Formation) deposited during the last glacial over the lake's shelf. Areas with significance level above 0.9 (alpha=0.1) are marked by a thick black line. Data is from (Kolodny et al., 2005).

https://doi.org/10.5194/cp-2020-161
Preprint. Discussion started: 11 January 2021

The North Atlantic (NAO) and the Eastern Atlantic (EA) oscillations are commonly considered as affecting interannual precipitation variability over the eastern Mediterranean (Feldstein, 2000; e.g., Feldstein and Dayan, 2008; Feliks et al., 2010; Krichak et al., 2002; Seager et al., 2019), primarily due to their reported effect on to discrete precipitation-bearing synoptic patterns over the eastern Mediterranean (e.g., Black, 2012). Others, on the other hand, have proposed that, unlike western Turkey, the direct impact of NAO on precipitation in the Levant is minimal (Enzel et al., 2003; Seager et al., 2020; Ziv et al., 2006). Although such relationships are hard to identify in geological records, a North Atlantic impact over the Dead Sea hydrology during the last glacial was identified at lower frequency by lake level reconstructions, where abrupt lake level drops were identified during Heinrich events (Bartov et al., 2003). Additionally, a NAO-like periodic component was also identified in laminated halite sequences during the last interglacial (Palchan et al., 2017). However, modern observations (Sirota et al., 2017), may indicate that this pacing is working through temperature variations, which bear significant implications on halite deposition, rather than through precipitation and hydrologic forcing.

Century-long precipitation data from the Kfar Giladi and Jerusalem stations correlate well with pre-regulated modern Dead Sea levels, and are thus considered as recorders of mean hydrological conditions over the northern and central Dead Sea watershed in recent and past times (Enzel et al., 2003; Morin et al., 2019). Thus, available records of annual precipitation and the number of annual rainy days in both stations were also compared here to winter (DJF) NAO and EA indices using wavelet and cross-wavelet spectra in order to detect common pacing and periodic components (Fig. S15 and S16; NOAA, 2020). Although these records are relatively short, spanning less than a century, they show little similarity with winter NAO and EA. However, short-term fluctuations with periodicity of 2-6 years were observed in the ICDP-DSDDP cores (Figs. 6, S6, S9-S14), in the isotopic composition of aragonite (Fig. 7; Kolodny et al., 2005), in modern precipitation records and in winter (DJF) NAO and EA (Figs. S15 and S16). This similarity, although not robust, could indeed point to a weak or non-linear effect of these teleconnections on precipitation in the eastern Mediterranean (e.g., Black, 2012). Alternatively, this can point to difficulties in extracting these delicate relationships from sedimentary archives that ultimately record a chain of processes and convoluted impacts of hydrological and limnological processes involved in laminae formation and post depositional changes; for example, these may include non-homogenous spread of fine-grained sediments over the lake floor and the effects of inflows from different catchments of multiple sizes as well as temperature.

5.3 Clusters and regime transitions

The studied episodes demonstrate pronounced clustering that emerged by the application of the Monte-Carlo based method that we developed to identify clusters of intense flooding (Appendix B). Similar, non-Poisson and non-uniform flood frequency distributions were also noted in other high-resolution palaeo-hydrological records (e.g., Witt et al., 2016) as well as modern flood data (Metzger et al., 2020). When this is considered together with reduced recurrence rate during clusters, the increased

https://doi.org/10.5194/cp-2020-161
Preprint. Discussion started: 11 January 2021

frequency of floods during clusters could be indicative of a hydroclimatic regime shift into a less persistent, possibly less-ordered or chaotic regime (Figs. 6-7). In addition, the clusters observed during lake level fall are characterized by flood frequencies similar to those of background episodes during lake level rise. This suggests that the wetter episodes are characterized by increased mean precipitation and variability, as well as increased frequency of intense storms, which is in agreement with modern and more recent observations (Morin et al., 2019).

The two clusters were identified in each of the studied late Pleistocene intervals, reveal opposing properties when their increased flood frequencies are compared with aragonite thicknesses. The opposing characteristics of the two clusters are evident by comparing their running mean (calculated as $RC^{(1)}$) and dispersion, calculated as the running standard deviation of the residuals (after subtracting $RC^{(1)}$) using a window of 30 years (Figs. S17 and S18). In each of the studied intervals, one cluster demonstrates increased mean and variance in both flood frequency and aragonite thickness, whereas the other cluster is characterized by increased mean flood frequency, but also by similar mean and variance of aragonite thickness (Figs. S19 and S20). Similarly, contrasting properties of the two clusters in each of the two intervals are revealed by their recurrence analyses, where one cluster shows a more pronounced drop in recurrence rate and transitivity than the other (Figs. 6-7). These two distinct approaches further demonstrate that the underlying processes responsible for each cluster are distinct, and in turn are also different from the background processes. Altogether, these observations call for a unified explanation that can account for this discrepancy in terms of hydroclimatic regimes and dominant synoptic circulation patterns.

Although modern records are relatively short, and the comparison of sparse hydrological measurements with the detailed framework of atmospheric circulation only permits cautious conclusions, the abovementioned observations can be explained using the modern synoptic framework by considering two distinct synoptic and hydroclimatic scenarios that govern flood formation and flood clustering over the catchments facing the ICDP-DSDDP coring site. Because most of the precipitation over the Dead Sea watershed is delivered by extra-tropical cyclones (Mediterranean lows) during winter months (e.g., Enzel et al., 2003; Saaroni et al., 2010; Ziv et al., 2006), when these cyclones are deep and characterized by a slightly southern track, they can pass slightly slower over the region and generate much more rainfall, and therefore they effectively deliver more precipitation to the watershed (e.g., Ben Dor et al., 2018; Ziv et al., 2006). Thus, they effectively increase annual precipitation, while increasing the chances of generating floods over the catchments that face the ICDP-DSDDP coring site (Armon et al., 2019; Belachsen et al., 2017; Goldreich et al., 2004). As suggested above, this scenario could account for the observed increase in both mean and variance of flood frequency and aragonite laminae thickness, observed in one of the clusters of each studied series (Fig. S19 and S20).

During the other cluster, on the other hand, the increased flood frequency is uncoupled with a clear increase in the mean and/or variance of the aragonite laminae thickness. Studies of modern floods and their synoptic settings suggest that floods can also be generated by other two synoptic systems: active Red Sea troughs (ARST) and jet stream disturbances (i.e., Tropical Plumes).

https://doi.org/10.5194/cp-2020-161
Preprint. Discussion started: 11 January 2021


Climate of the Past Discussions

These synoptic conditions can generate significant floods over the small catchments surrounding the ICDP-DSDDP coring site, thus having the potential to deliver sediments, but because of their spatiotemporal properties and frequency, would have negligible contribution to total inflow into the lake (Armon et al., 2019). However, in present-day ARSTs are more frequent than Tropical Plumes, and are characterized by high peak discharge and relatively low volume floods (Armon et al., 2018; Shentsis et al., 2012) the second cluster may be thus explained by increased ARST frequency. This would lead to increased flood frequency (more sub-laminae) without drastically increasing annual inflow (similar aragonite thickness).

6 Conclusions

The short-term hydroclimatic variability of opposing climatic trends in the Levant was studied using multiple statistical analyses of two annually-resolved varve sequences of the ICDP-DSDDP cores, representing opposing mean climates recorded by contrasting lake level trends. This unique sedimentary record complements the otherwise short and sparse modern climatic and hydrological records; it adds aspects and properties of longer time series of regional hydroclimatology. By the analyses of two distinct sedimentary proxies that reflect annual inflow and flood frequency, and by their comparison with modern climatic data from a synoptic perspective, new insights on hydroclimatic stationarity during late Pleistocene climate changes are revealed. These findings improve our understanding of short-term late Pleistocene hydroclimatic variability; moreover, they point to factors pacing hydroclimatic aspects and periodic components. Several conclusions arise:

1. The dispersion of aragonite laminae thickness and flood frequency in the ICDP-DSDDP cores are fairly correlated with their corresponding mean, similar to modern hydrologic observations. These findings strengthen the interpretation of these proxies as recorders of hydroclimatic phenomena in the Dead Sea watershed. During the "wetter" interval characterized by lake level rise, both the mean and the variance of these proxies are larger than during the studied episode of falling lake level.
2. Singular spectrum, wavelet and recurrence analyses reveal short-term quasi-periodical components that affect annual precipitation and flood frequency during the late Pleistocene. Although the inherent link between aragonite thickness and annual inflow is probably not linear, the two proxies show similar periodical components of 2-3, 4-5, and 7-8 years, that could stem from the interaction of quasi-periodic ~3-4 years components, possibly related to the North Atlantic Oscillation.

Flood frequencies over the studied series demonstrate strong hydro-climatological regime shifts operating at a centennial time scale. The clusters show distinct characteristics in terms of the relationship between mean and dispersion of flood frequency and annual inflow. Namely, in each studied series one cluster is characterized by increased mean and variance of the two proxies, whereas the other one shows increased mean and variance only in flood frequency but not in annual precipitation. This implies that the clusters were generated by distinct hydroclimatic regimes characterized by different relative dominance of various synoptic systems that lead to increased floods frequency at a decadal-scale. Such regime shifts could also affect modern or future conditions that would manifest as drastic hydroclimatic shifts at decadal to centennial scales.

https://doi.org/10.5194/cp-2020-161
Preprint. Discussion started: 11 January 2021

7 Appendices

See attached file

Supplementary 1– figures

Supplementary 2 – non-parametric test developed for identifying clusters

8 Code availability

All code that was used for this research is available upon request from the corresponding author.

9 Data availability

All the data that was used for this research is available in the appendices or upon request from the corresponding author.

10 Competing interests

The authors declare that they have no conflict of interest.

Acknowledgements

This study is a contribution to the PALEX project "Paleohydrology and Extreme Floods from the Dead Sea ICDP core", funded by the DFG to A. Brauer, Y. Enzel, E. Morin, and Y. Erel (grant no. BR2208/13-1/-2). The authors acknowledge the support and contribution of laboratory staff and technicians in the GFZ, where preparation of thin-sections and photography were carried. We thank J. Mingram, N. Nowaczyk, B. Brademann, F. Ott, N. Dräger and M. Köppel for technical support and fruitful discussions. Y.B. is also grateful for a scholarship from the Advanced School of Environmental Studies, the Hebrew University of Jerusalem, and from the Rieger Foundation-Jewish National Fund program for environmental studies.

References

Ahlborn, M., Armon, M., Ben Dor, Y., Neugebauer, I., Schwab, M. J., Tjallingii, R., Shoqeir, J. H., Morin, E., Enzel, Y. and Brauer, A.: Increased frequency of torrential rainstorms during a regional late Holocene eastern Mediterranean drought, Quat. Res. (United States), 89(2), doi:10.1017/qua.2018.9, 2018.

Allen, K. J., Hope, P., Lam, D., Brown, J. R. and Wasson, R. J.: Improving Australia's flood record for planning purposes–can we do better?, Aust. J. Water Resour., 00(00), 1–10, doi:10.1080/13241583.2020.1745735, 2020.

Alpert, P., Ben-Gai, T., Baharad, A., Benjamini, Y., Yekutieli, D., Colacino, M., Diodato, L., Ramis, C., Homar, V., Romero, R., Michaelides, S. and Manes, A.: The paradoxical increase of Mediterranean extreme daily rainfall in spite of decrease in

https://doi.org/10.5194/cp-2020-161
Preprint. Discussion started: 11 January 2021

total values, Geophys. Res. Lett., 29(11), 31-1-31–4, doi:10.1029/2001GL013554, 2002.

Ansari, A. R. and Bradley, R. A.: Rank-Sum Tests for Dispersions, Ann. Math. Stat., 31(4), 1174–1189 [online] Available from: https://www.jstor.org/stable/pdf/2237814.pdf?refreqid=excelsior%3A3d25ddb377eecec2621e692b57882f61, 1960.

Armon, M., Dente, E., Smith, J. A., Enzel, Y. and Morin, E.: Synoptic-scale control over modern rainfall and flood patterns in the Levant drylands with implications for past climates, J. Hydrometeorol., 19(6), 1077–1096, doi:10.1175/JHM-D-18-0013.1, 2018.

Armon, M., Morin, E. and Enzel, Y.: Overview of modern atmospheric patterns controlling rainfall and floods into the Dead Sea: Implications for the lake's sedimentology and paleohydrology, Quat. Sci. Rev., 216, 58–73, doi:10.1016/j.quascirev.2019.06.005, 2019.

Baker, V. R.: Paleoflood hydrology: Origin, progress, prospects, Geomorphology, 101(1–2), 1–13, doi:10.1016/j.geomorph.2008.05.016, 2008.

Bartov, Y., Stein, M., Enzel, Y., Agnon, A. and Reches, Z.: Lake levels and sequence stratigraphy of Lake Lisan, the late Pleistocene precursor of the Dead Sea, Quat. Res., 57(1), 9–21, doi:10.1006/qres.2001.2284, 2002.

Bartov, Y., Goldstein, S. J., Stein, M. and Enzel, Y.: Catastrophic aid episodes in the Eastern Mediterranean linked with the North Atlantic Heinrich events, Geology, 31(5), 439–442, doi:10.1130/0091-7613(2003)031<0439:CAEITE>2.0.CO;2, 2003.

Bartov, Y., Enzel, Y., Porat, N. and Stein, M.: Evolution of the Late Pleistocene Holocene Dead Sea Basin from Sequence Statigraphy of Fan Deltas and Lake-Level Reconstruction, J. Sediment. Res., 77(9), 680–692, doi:10.2110/jsr.2007.070, 2007.

Begin, Z. B., Nathan, Y. and Ehrlich, A.: Stratigraphy and facies distribution in the Lisan Formation—new evidence from the area south of the Dead Sea, Israel, Isr. J. Earth Sci., 29, 182–189, 1980.

Begin, Z. B., Stein, M., Katz, A., Machlus, M., Rosenfeld, A., Buchbinder, B. and Bartov, Y.: Southward migration of rain tracks during the last glacial, revealed by salinity gradient in Lake Lisan (Dead Sea rift), Quat. Sci. Rev., 23(14–15), 1627–1636, doi:10.1016/j.quascirev.2004.01.002, 2004.

Belachsen, I., Marra, F., Peleg, N. and Morin, E.: Convective rainfall in a dry climate: Relations with synoptic systems and flash-flood generation in the Dead Sea region, Hydrol. Earth Syst. Sci., 21(10), 5165–5180, doi:10.5194/hess-21-5165-2017, 2017.

Black, E.: The influence of the North Atlantic Oscillation and European circulation regimes on the daily to interannual variability of winter precipitation in Israel, Int. J. Climatol., 32(11), 1654–1664, doi:10.1002/joc.2383, 2012.

Blackman, R. B. and Tukey, J. W.: The Measurement of Power Spectra from the Point of View of Communications Engineering — Part II, Bell Syst. Tech. J., 37(2), 485–569, doi:10.1002/j.1538-7305.1958.tb01530.x, 1958.

Bookman, R., Bartov, Y., Enzel, Y. and Stein, M.: Quaternary lake levels in the Dead Sea basin: Two centuries of research, Spec. Pap. Geol. Soc. Am., 401(10), 155–170, doi:10.1130/2006.2401(10), 2006.

Brauer, A., Endres, C., Günter, C., Litt, T., Stebich, M. and Negendank, J. F. W.: High resolution sediment and vegetation responses to Younger Dryas climate change in varved lake sediments from Meerfelder Maar, Germany, Quat. Sci. Rev., 18(3), 321–329, doi:10.1016/S0277-3791(98)00084-5, 1999.

https://doi.org/10.5194/cp-2020-161
Preprint. Discussion started: 11 January 2021

Brauer, A., Mangili, C., Moscariello, A. and Witt, A.: Palaeoclimatic implications from micro-facies data of a 5900 varve time series from the Piànico interglacial sediment record, southern Alps, Palaeogeogr. Palaeoclimatol. Palaeoecol., 259(2–3), 121–135, doi:10.1016/j.palaeo.2007.10.003, 2008.

Broomhead, D. S. and King, G. P.: Extracting qualitative dynamics from experimental data, Phys. D Nonlinear Phenom., 20(2–3), 217–236, doi:10.1016/0167-2789(86)90031-X, 1986.

Campins, J., Genovés, A., Picornell, M. A. and Jansà, A.: Climatology of Mediterranean cyclones using the ERA-40 dataset, Int. J. Climatol., 31(11), 1596–1614, doi:10.1002/joc.2183, 2011.

Coianiz, L., Ben-Avraham, Z., Stein, M. and Lazar, M.: Spatial and temporal reconstruction of the late Quaternary Dead Sea sedimentary facies from geophysical properties, J. Appl. Geophys., 160, 15–27, doi:10.1016/j.jappgeo.2018.11.002, 2019.

David-Novak, H. Ben, Morin, E. and Enzel, Y.: Modern extreme storms and the rainfall thresholds for initiating debris flow on the hyperarid western escarpment of the Dead Sea, Israel, Bull. Geol. Soc. Am., 116(5–6), 718–728, doi:10.1130/B25403.2, 2004.

Dayan, U. and Morin, E.: Flash flood – producing rainstorms over the Dead Sea: A review, New Front. Dead Sea …, 2401(04), 53–62, doi:10.1130/2006.2401(04)., 2006.

Donges, J. F., Donner, R. V., Trauth, M. H., Marwan, N., Schellnhuber, H. J. and Kurths, J.: Nonlinear detection of paleoclimate-variability transitions possibly related to human evolution, Proc. Natl. Acad. Sci. U. S. A., 108(51), 20422–20427, doi:10.1073/pnas.1117052108, 2011.

Ben Dor, Y., Armon, M., Ahlborn, M., Morin, E., Erel, Y., Brauer, A., Schwab, M. J. M. J., Tjallingii, R. and Enzel, Y.: Changing flood frequencies under opposing late Pleistocene eastern Mediterranean climates, Sci. Rep., 8(1), 1–10, doi:10.1038/s41598-018-25969-6, 2018.

Ben Dor, Y., Neugebauer, I., Enzel, Y., Schwab, M. J., Tjallingii, R., Erel, Y. and Brauer, A.: Varves of the Dead Sea sedimentary record, Quat. Sci. Rev., 215, 173–184, doi:10.1016/j.quascirev.2019.04.011, 2019.

Eckmann, J. P., Oliffson Kamphorst, O. and Ruelle, D.: Recurrence plots of dynamical systems, Epl, 4(9), 973–977, doi:10.1209/0295-5075/4/9/004, 1987.

Enzel, Y., Bookman (Ken Tor), R., Sharon, D., Gvirtzman, H., Dayan, U., Ziv, B. and Stein, M.: Late Holocene climates of the Near East deduced from Dead Sea level variations and modern regional winter rainfall, Quat. Res., 60(3), 263–273, doi:10.1016/j.yqres.2003.07.011, 2003.

Enzel, Y., Amit, R., Dayan, U., Crouvi, O., Kahana, R., Ziv, B. and Sharon, D.: The climatic and physiographic controls of the eastern Mediterranean over the late Pleistocene climates in the southern Levant and its neighboring deserts, Glob. Planet. Change, 60(3–4), 165–192, doi:10.1016/j.gloplacha.2007.02.003, 2008.

Enzel, Y., Amit, R., Grodek, T., Ayalon, A., Lekach, J., Porat, N., Bierman, P., Blum, J. D. and sErel, Y.: Late Quaternary weathering, erosion, and deposition in Nahal Yael, Israel: An “impact of climatic change on an arid watershed”?, Bull. Geol. Soc. Am., 124(5–6), 705–722, doi:10.1130/B30538.1, 2012.

Feldstein, S. B.: The Timescale, Power Spectra, and Climate Noise Properties of Teleconnection Patterns, American

https://doi.org/10.5194/cp-2020-161
Preprint. Discussion started: 11 January 2021

Meteorological Society., 2000.

Feldstein, S. B. and Dayan, U.: Circumglobal teleconnections and wave packets associated with Israeli winter precipitation, Q. J. R. Meteorol. Soc., 134(631), 455–467, doi:10.1002/qj.225, 2008.

Feliks, Y., Ghil, M. and Robertson, A. W.: Oscillatory climate modes in the eastern Mediterranean and their synchronization with the North Atlantic Oscillation, J. Clim., 23(15), 4060–4079, doi:10.1175/2010JCLI3181.1, 2010.

Flocas, H. A., Simmonds, I., Kouroutzoglou, J., Keay, K., Hatzaki, M., Bricolas, V. and Asimakopoulos, D.: On cyclonic tracks over the Eastern Mediterranean, J. Clim., 23(19), 5243–5257, doi:10.1175/2010JCLI3426.1, 2010.

Garber, R. A., Levy, Y. and Friedman, G. M.: The sedimentology of the Dead Sea, Carbonates and Evaporites, 2(1), 43–57, doi:10.1007/BF03174303, 1987.

Garfunkel, Z.: Internal structure of the Dead Sea leaky transform (rift) in relation to plate kinematics, Tectonophysics, 80(1–4), 81–108, doi:10.1016/0040-1951(81)90143-8, 1981.

Garfunkel, Z. and Ben-Avraham, Z.: The structure of the Dead Sea basin, Tectonophysics, 266(1–4), 155–176, doi:10.1016/S0040-1951(96)00188-6, 1996.

Ghil, M., Allen, M. R., Dettinger, M. D., Ide, K., Kondrashov, D., Mann, M. E., Robertson, A. W., Saunders, A., Tian, Y., Varadi, F. and Yiou, P.: Advanced spectral methods for climatic time series, Rev. Geophys., 40(1), 3-1-3–41, doi:10.1029/2000RG000092, 2002.

Goldreich, Y., Mozes, H. and Rosenfeld, D.: Radar analysis of cloud systems and their rainfall yield in Israel, Isr. J. Earth Sci., 53(2), 63–76, doi:10.1560/G68K-30MN-D5V0-KUHU, 2004.

Greenbaum, N., Schwartz, U. and Bergman, N.: Extreme floods and short-term hydroclimatological fluctuations in the hyper-arid Dead Sea region, Israel, Glob. Planet. Change, 70(1–4), 125–137, doi:10.1016/j.gloplacha.2009.11.013, 2010.

Grinsted, A., Moore, J. C. and Jevrejeva, S.: Application of the cross wavelet transform and wavelet coherence to geophysical time series, Nonlinear Process. Geophys., 11(5/6), 561–566, doi:10.5194/npg-11-561-2004, 2004.

Groth, A. and Ghil, M.: Monte Carlo singular spectrum analysis (SSA) revisited: Detecting oscillator clusters in multivariate datasets, J. Clim., 28(19), 7873–7893, doi:10.1175/JCLI-D-15-0100.1, 2015.

Haase-Schramm, A., Goldstein, S. L. and Stein, M.: U-Th dating of Lake Lisan (late Pleistocene dead sea) aragonite and implications for glacial east Mediterranean climate change, Geochim. Cosmochim. Acta, 68(5), 985–1005, doi:10.1016/j.gca.2003.07.016, 2004.

Heim, C., Nowaczyk, N. R., Negendank, J. F. W., Leroy, S. A. G. and Ben-Avraham, Z.: Near East desertification: Evidence from the Dead Sea, Naturwissenschaften, 84(9), 398–401, doi:10.1007/s001140050416, 1997.

Held, I. M. and Soden, B. J.: Robust responses of the hydrological cycle to global warming, J. Clim., 19(21), 5686–5699, doi:10.1175/JCLI3990.1, 2006.

Kagan, E., Stein, M. and Marco, S.: Integrated Paleoseismic Chronology of the Last Glacial Lake Lisan: From Lake Margin Seismites to Deep-Lake Mass Transport Deposits, J. Geophys. Res. Solid Earth, 123(4), 2806–2824, doi:10.1002/2017JB014117, 2018.

https://doi.org/10.5194/cp-2020-161
Preprint. Discussion started: 11 January 2021

Kahana, R., Ziv, B., Enzel, Y. and Dayan, U.: Synoptic climatology of major floods in the Negev Desert, Israel, Int. J. Climatol., 22(7), 867–882, doi:10.1002/joc.766, 2002.

Kelley, C., Ting, M., Seager, R. and Kushnir, Y.: Mediterranean precipitation climatology, seasonal cycle, and trend as simulated by CMIP5, Geophys. Res. Lett., 39(21), 1–7, doi:10.1029/2012GL053416, 2012.

Kennel, M. B., Brown, R. and Abarbanel, H. D. I.: Determining embedding dimension for phase-space reconstruction using a geometrical construction, Phys. Rev. A, 45(6), 3403–3411, doi:10.1103/PhysRevA.45.3403, 1992.

Kiro, Y., Goldstein, S. L., Lazar, B. and Stein, M.: Environmental implications of salt facies in the Dead Sea, Geol. Soc. Am. Bull., 128(5–6), 824–841, doi:10.1130/b31357.1, 2016.

Kolodny, Y., Stein, M. and Machlus, M.: Sea-rain-lake relation in the Last Glacial East Mediterranean revealed by δ18O-δ13C in Lake Lisan aragonites, Geochim. Cosmochim. Acta, 69(16), 4045–4060, doi:10.1016/j.gca.2004.11.022, 2005.

Krichak, S. O., Kishcha, P. and Alpert, P.: Decadal trends of main Eurasian oscillations and the eastern Mediterranean precipitation, Theor. Appl. Climatol., 72(3–4), 209–220, doi:10.1007/s007040200021, 2002.

Kushnir, Y., Dayan, U., Ziv, B., Morin, E. and Enzel, Y.: Climate of the Levant, Quat. Levant, 31–44, doi:10.1017/9781316106754.004, 2017.

Lau, K. M. and Hengyi Weng: Climate signal detection using wavelet transform: how to make a time series sing, Bull. - Am. Meteorol. Soc., 76(12), 2391–2402, doi:10.1175/1520-0477(1995)076<2391:CSDUWT>2.0.CO;2, 1995.

Luck, M., Landis, M. and Gassert, F.: Aqueduct Water Stress Projections: Decadal projections of water supply and demand using CMIP5 GCMs., World Resour. Inst. Techical Note, (April), 1–20 [online] Available from: wri.org/publication/aqueduct-water-stress-projections, 2015.

Luo, T., Young, R. and Reig., P.: Aqueduct Projected Water Stress Country Rankings. Technical Note. Washington, D.C.: World Resources Institute, , (August), 1–16, 2015.

Machlus, M., Enzel, Y., Goldstein, S. L., Marco, S. and Stein, M.: Reconstructing low levels of Lake Lisan by correlating fan-delta and lacustrine deposits, Quat. Int., 73–74, 137–144, doi:10.1016/S1040-6182(00)00070-7, 2000.

Mann, H. B. and Whitney, D. R.: On a Test of Whether one of Two Random Variables is Stochastically Larger than the Other, Ann. Math. Stat., 18(1), 50–60 [online] Available from: https://www.jstor.org/stable/pdf/2236101.pdf, 1947.

Marwan, N.: How to avoid potential pitfalls in recurrence plot based data analysis, Int. J. Bifurc. Chaos, 21(4), 1003–1017, doi:10.1142/S0218127411029008, 2011.

Marwan, N. and Kurths, J.: Cross Recurrence Plots and Their Applications, Math. Phys. Res. Cut. Edge, 101–139, doi:10.1093/brain/aws023, 2004.

Marwan, N., Trauth, M. H., Vuille, M. and Kurths, J.: Comparing modern and Pleistocene ENSO-like influences in NW Argentina using nonlinear time series analysis methods, Clim. Dyn., 21(3–4), 317–326, doi:10.1007/s00382-003-0335-3, 2003.

Marwan, N., Carmen Romano, M., Thiel, M. and Kurths, J.: Recurrence plots for the analysis of complex systems, Phys. Rep., 438(5–6), 237–329, doi:10.1016/j.physrep.2006.11.001, 2007.

https://doi.org/10.5194/cp-2020-161
Preprint. Discussion started: 11 January 2021

Metzger, A., Marra, F., Smith, J. A. and Morin, E.: Flood frequency estimation and uncertainty in arid/semi-arid regions, J. Hydrol., 590, 125254, doi:10.1016/j.jhydrol.2020.125254, 2020.

Migowski, C., Stein, M., Prasad, S., Negendank, J. F. W. and Agnon, A.: Holocene climate variability and cultural evolution in the Near East from the Dead Sea sedimentary record, Quat. Res., 66(3), 421–431, doi:10.1016/j.yqres.2006.06.010, 2006.

Morin, E.: To know what we cannot know: Global mapping of minimal detectable absolute trends in annual precipitation, Water Resour. Res., 47(7), doi:10.1029/2010WR009798, 2011.

Morin, E., Ryb, T., Gavrieli, I. and Enzel, Y.: Mean, variance, and trends of Levant precipitation over the past 4500 years from reconstructed Dead Sea levels and stochastic modeling, Quat. Res. (United States), 91(2), 751–767, doi:10.1017/qua.2018.98, 2019.

Le Mouël, J. L., Lopes, F. and Courtillot, V.: A Solar Signature in Many Climate Indices, J. Geophys. Res. Atmos., 124(5), 2600–2619, doi:10.1029/2018JD028939, 2019.

Neev, D.: Recent precipitation of calcium salts in the Dead Sea, in Israel Research Council Bulletin, pp. 153–154., 1963.

Neev, D. and Emery, K. O.: The Dead Sea: depositional processes and environments of evaporites, Isr. Geol. Surv. Bull., 41, 1–47, 1967.

Nehorai, R., Lensky, I. M., Hochman, L., Gertman, I., Brenner, S., Muskin, A. and Lensky, N. G.: Satellite observations of turbidity in the Dead Sea, J. Geophys. Res. Ocean., 118(6), 3146–3160, doi:10.1002/jgrc.20204, 2013.

Neugebauer, I., Brauer, A., Schwab, M. J., Waldmann, N. D., Enzel, Y., Kitagawa, H., Torfstein, A., Frank, U., Dulski, P., Agnon, A., Ariztegui, D., Ben-Avraham, Z., Goldstein, S. L. and Stein, M.: Lithology of the long sediment record recovered by the ICDP Dead Sea Deep Drilling Project (DSDDP), Quat. Sci. Rev., 102, 149–165, doi:10.1016/j.quascirev.2014.08.013, 2014.

Neugebauer, I., Brauer, A., Schwab, M. J., Dulski, P., Frank, U., Hadzhiivanova, E., Kitagawa, H., Litt, T., Schiebel, V., Taha, N. and Waldmann, N. D.: Evidences for centennial dry periods at ~3300 and ~2800 cal. yr BP from micro-facies analyses of the Dead Sea sediments, Holocene, 25(8), 1358–1371, doi:10.1177/0959683615584208, 2015.

Nissenbaum, A., Baedecker, M. J. and Kaplan, I. R.: Organic geochemistry of Dead Sea sediments, Geochim. Cosmochim. Acta, 36(7), 709–727, doi:10.1016/0016-7037(72)90082-8, 1972.

NOAA: Climate Prediction Center, [online] Available from: https://www.cpc.ncep.noaa.gov/data/teledoc/ea.shtml (Accessed 29 July 2020), 2020.

Palchan, D., Neugebauer, I., Amitai, Y., Waldmann, N. D., Schwab, M. J., Dulski, P., Brauer, A., Stein, M., Erel, Y. and Enzel, Y.: North Atlantic controlled depositional cycles in MIS 5e layered sediments from the deep Dead Sea basin, Quat. Res. (United States), 87(1), 168–179, doi:10.1017/qua.2016.10, 2017.

Peleg, N., Bartov, M. and Morin, E.: CMIP5-predicted climate shifts over the East Mediterranean: Implications for the transition region between Mediterranean and semi-arid climates, Int. J. Climatol., 35(8), 2144–2153, doi:10.1002/joc.4114, 2015.

Prasad, S., Vos, H., Negendank, J. F. W., Waldmann, N., Goldstein, S. L. and Stein, M.: Evidence from Lake Lisan of solar

https://doi.org/10.5194/cp-2020-161
Preprint. Discussion started: 11 January 2021

influence on decadal- To centennial-scale climate variability during marine oxygen isotope stage 2, Geology, 32(7), 581–584, doi:10.1130/G20553.1, 2004.

Redmond, K. T., Enzel, Y., House, P. K. and Biondi, F.: Climate variability and flood frequency at decadal to millennial time scales, Anc. floods, Mod. hazards Princ. Appl. paleoflood Hydrol., 5, 21–45, 2002.

Rohling, E. J.: Quantitative assessment of glacial fluctuations in the level of Lake Lisan, Dead Sea rift, Quat. Sci. Rev., 70, 63–72, doi:https://doi.org/10.1016/j.quascirev.2013.03.013, 2013.

Saaroni, H., Halfon, N., Ziv, B., Alpert, P. and Kutiel, H.: Links between the rainfall regime in Israel and location and intensity of Cyprus lows, Int. J. Climatol., 30(7), 1014–1025, doi:10.1002/joc.1912, 2010.

Safriel, U., Adeel, Z., Niemeijer, D., Puigdefabregas, J., White, R., Lal, R., Winslow, M., Ziedler, J., Prince, S., Archer, E., King, C., Shapiro, B., Wessels, K., Nielsen, T. T., Portnov, B., Reshef, I., Thornell, J., Lachman, E. and McNab, D.: Dryland systems, , 623–662 [online] Available from: https://forskning.ruc.dk/en/publications/dryland-systems (Accessed 27 August 2020), 2005.

Seager, R., Osborn, T. J., Kushnir, Y., Simpson, I. R., Nakamura, J. and Liu, H.: Climate variability and change of mediterranean-type climates, J. Clim., 32(10), 2887–2915, doi:10.1175/JCLI-D-18-0472.1, 2019.

Seager, R., Liu, H., Kushnir, Y., Osborn, T. J., Simpson, I. R., Kelley, C. R. and Nakamura, J.: Mechanisms of Winter Precipitation Variability in the European–Mediterranean Region Associated with the North Atlantic Oscillation, J. Clim., 33(16), 7179–7196, doi:10.1175/JCLI-D-20-0011.1, 2020.

Serinaldi, F., Kilsby, C. G. and Lombardo, F.: Untenable nonstationarity: An assessment of the fitness for purpose of trend tests in hydrology, Adv. Water Resour., 111, 132–155, doi:10.1016/j.advwatres.2017.10.015, 2018.

Shentsis, I., Laronne, J. B. and Alpert, P.: Red Sea Trough flood events in the Negev, Israel (1964-2007), Hydrol. Sci. J., 57(1), 42–51, doi:10.1080/02626667.2011.636922, 2012.

Shohami, D., Dayan, U. and Morin, E.: Warming and drying of the eastern Mediterranean: Additional evidence from trend analysis, J. Geophys. Res. Atmos., 116(22), 1–12, doi:10.1029/2011JD016004, 2011.

Sirota, I., Enzel, Y. and Lensky, N. G.: Temperature seasonality control on modern halite layers in the Dead Sea: In situ observations, Bull. Geol. Soc. Am., 129(9–10), 1181–1194, doi:10.1130/B31661.1, 2017.

Stein, M., Starinsky, A., Katz, A., Goldstein, S. L., Machlus, M. and Schramm, A.: Strontium isotopic, chemical, and sedimentological evidence for the evolution of Lake Lisan and the Dead Sea, Geochim. Cosmochim. Acta, 61(18), 3975–3992, doi:10.1016/S0016-7037(97)00191-9, 1997.

Stein, M., Ben-Avraham, Z. and Goldstein, S. L.: Dead Sea Deep Cores: A Window A Library of Georeferenced Into Past Climate and Seismicity, Eos (Washington. DC)., 92(49), 453–454, doi:10.1111/j.2006.0906-7590.04596.x.Xiao, 2011.

Stöckli, R., Vermote, E., Saleous, N., Simmon, R. and Herring, D.: The Blue Marble Next Generation-A true color earth dataset including seasonal dynamics from MODIS, Publ. by NASA Earth Obs., 2005.

Swierczynski, T., Brauer, A., Lauterbach, S., Martín-Puertas, C., Dulski, P., von Grafenstein, U. and Rohr, C.: A 1600 yr seasonally resolved record of decadal-scale flood variability from the Austrian Pre-Alps, Geology, 40(11), 1047–1050,

705 doi:10.1130/G33493.1, 2012.

Tamarin-Brodsky, T. and Kaspi, Y.: Enhanced poleward propagation of storms under climate change, Nat. Geosci., 10(12), 908–913, doi:10.1038/s41561-017-0001-8, 2017.

Tarolli, P., Borga, M., Morin, E. and Delrieu, G.: Analysis of flash flood regimes in the North-Western and South-Eastern Mediterranean regions, Nat. Hazards Earth Syst. Sci., 12(5), 1255–1265, doi:10.5194/nhess-12-1255-2012, 2012.

710 Torfstein, a., Gavrieli, I., Katz, a., Kolodny, Y. and Stein, M.: Gypsum as a monitor of the paleo-limnological-hydrological conditions in Lake Lisan and the Dead Sea, Geochim. Cosmochim. Acta, 72(10), 2491–2509, doi:10.1016/j.gca.2008.02.015, 2008.

Torfstein, A.: Brine freshwater interplay and effects on the evolution of saline lakes : The Dead Sea Rift terminal lakes by Brine freshwater interplay and effects on the evolution of saline lakes : The Dead Sea Rift terminal lakes, , (August), 2008.

715 Torfstein, A. and Enzel, Y.: Dead Sea Lake Level Changes and Levant Palaeoclimate, in Quaternary of the Levant: Environments, Climate Change, and Humans, pp. 115–126., 2017.

Torfstein, A., Haase-Schramm, A., Waldmann, N., Kolodny, Y. and Stein, M.: U-series and oxygen isotope chronology of the mid-Pleistocene Lake Amora (Dead Sea basin), Geochim. Cosmochim. Acta, 73(9), 2603–2630, doi:10.1016/j.gca.2009.02.010, 2009.

720 Torfstein, A., Goldstein, S. L., Kagan, E. J. and Stein, M.: Integrated multi-site U – Th chronology of the last glacial Lake Lisan, Geochim. Cosmochim. Acta, 104, 210–231, doi:10.1016/j.gca.2012.11.003, 2013.

Torrence, C. and Compo, G. P.: A practical guide to wavelet analysis, Bull. Am. Meteorol. Soc., 79(1), 61–78, doi:10.1175/1520-0477(1998)079<0061:APGTWA>2.0.CO;2, 1998.

Tsvieli, Y. and Zangvil, A.: Synoptic climatological analysis of "wet" and "dry" Red Sea Troughs over Israel, Int. J. Climatol.,

725 25(15), 1997–2015, doi:10.1002/joc.1232, 2005.

Tubi, A. and Dayan, U.: Tropical Plumes over the Middle East: Climatology and synoptic conditions, Atmos. Res., 145–146, 168–181, doi:10.1016/j.atmosres.2014.03.028, 2014.

Vautard, R. and Ghil, M.: Singular spectrum analysis in nonlinear dynamics, with applications to paleoclimatic time series, Phys. D Nonlinear Phenom., 35(3), 395–424, doi:10.1016/0167-2789(89)90077-8, 1989.

730 Waldmann, N.: The Stratigraphy and Chronology of the Samra Formation, in Quaternary of the Levant: Environments, Climate Change, and Humans, edited by O. Bar-Yosef and Y. Enzel, pp. 99–106, Cambridge University Press, Cambridge., 2017.

Waldmann, N., Neugebauer, I., Palchan, D., Hadzhiivanova, E., Taha, N., Brauer, A. and Enzel, Y.: Sedimentology of the Lacustrine Formations in the Dead Sea Basin, Quat. Levant, 83–90, doi:10.1017/9781316106754.009, 2017.

Welch, P. D.: Welchs Periodogram.pdf, IEEE Trans. Audio Electroacoust., 15, 70–73, 1967.

735 Witt, A., Malamud, B. D., Mangili, C. and Brauer, A.: Analysis and Modelling of a 9.3 kyr Palaeoflood Record: Correlations, Clustering and Cycles, Hydrol. Earth Syst. Sci. Discuss., (October), 1–60, doi:10.5194/hess-2016-470, 2016.

Yosef, Y., Aguilar, E. and Alpert, P.: Changes in extreme temperature and precipitation indices: Using an innovative daily homogenized database in Israel, Int. J. Climatol., 39(13), 5022–5045, doi:10.1002/joc.6125, 2019.

https://doi.org/10.5194/cp-2020-161
Preprint. Discussion started: 11 January 2021

Zappa, G., Hawcroft, M. K., Shaffrey, L., Black, E. and Brayshaw, D. J.: Extratropical cyclones and the projected decline of winter Mediterranean precipitation in the CMIP5 models, Clim. Dyn., 45(7–8), 1727–1738, doi:10.1007/s00382-014-2426-8, 2015.

Ziv, B.: A subtropical rainstorm associated with a tropical plume over Africa and the Middle-East, Theor. Appl. Climatol., 69(1–2), 91–102, doi:10.1007/s007040170037, 2001.

Ziv, B., Saaroni, H. and Alpert, P.: The factors governing the summer regime of the eastern Mediterranean, Int. J. Climatol., 24(14), 1859–1871, doi:10.1002/joc.1113, 2004.

Ziv, B., Dayan, U., Kushnir, Y., Roth, C. and Enzel, Y.: Regional and global atmospheric patterns governing rainfall in the southern Levant, Int. J. Climatol., 26(1), 55–73, doi:10.1002/joc.1238, 2006.

Zolitschka, B., Francus, P., Ojala, A. E. K. and Schimmelmann, A.: Varves in lake sediments - a review, Quat. Sci. Rev., 117, 1–41, doi:10.1016/j.quascirev.2015.03.019, 2015.